Terr. Atmos. Ocean. Sci., Vol. 28, No. 3, 193-207, June 2017 doi: 10.3319/TAO.2015.09.21.02(GSC)

Rock core-based pre-stress evaluation experimental validation: A case study on Yutengping Sandstone as CO_2 storage reservoir rock

Jian-Hong Wu *, Hung-Ming Lin, and Yu-You Chen

Department of Civil Engineering, National Cheng Kung University, Tainan City, Taiwan

Article history:

Received 2 February 2012
Revised 10 June 2012
Accepted 21 September 2015

Keywords:

Geological CO_2 storage, Acoustic emission, Deformation rate analysis, Pre-stress, Yutengping Sandstone, Tieh-chan-shan

Citation:

Wu, J.-H., H.-M. Lin, and Y.-Y. Chen, 2017: Rock core-based pre-stress evaluation experimental validation: A case study on Yutengping Sandstone as CO_2 storage reservoir rock. Terr. Atmos. Ocean. Sci., 28, 193-207, doi: 10.3319/TAO.2015.09.21.02(GSC)

ABSTRACT

Yutengping Sandstone in Tieh-chan-shan, Taiwan is a potential reservoir for geological CO_2 storage. Cyclic loadings were applied to rock samples taken from an outcrop to create artificial pre-stress. The pre-stress evaluation accuracies using two core-based techniques, acoustic emission (AE) and deformation rate analysis (DRA), were investigated under different pre-stresses, delay times and curing temperatures. The experimental results validate the pre-stress evaluations using AE and DRA. The delay time and curing temperature were shown to have minor impacts on the measurement accuracy. However, although both axial strain and lateral strain can be used in DRA, the stress memory fades as the delay time increases. Therefore, delay time, which represents the time from the borehole drilling to the DRA test, must be carefully considered when applying these techniques to evaluate the *in situ* stress of Yutengping sandstone.

1. INTRODUCTION

The injection pressure and rate at a CO_2 injection site must be sufficiently high to accommodate the injection of a desired yearly mass of CO_2. The ability of the reservoir rock to contain the injected CO_2 is determined by measuring artificial pressure exceeding the initial reservoir pressure. During CO_2 injection the increasing reservoir fluid pressure induces mechanical deformations and stresses in and around the injection formation. If the reservoir pressure becomes too high the induced stresses may create new cracks or reactivate existing faults (Streit and Hillis 2004; Cailly et al. 2005; Rutqvist et al. 2007).

Figure 1 shows the relationship between the failure criteria of intact/jointed rock and the Mohr circles of the *in situ* stresses. In the analytical shear-slip analysis when the fluid CO_2 is injected into the rock mass the increasing pore pressure moves the effective-stress Mohr-circle with an identical diameter to the left, approaching the failure criteria (Fig. 1a). However, if thermal- or poro-elastic stressing is assumed during CO_2 injection, the diameter of the effective-stress Mohr-circle increases while the effective stress decreases (Fig. 1b). Therefore, the *in situ* stress of the reservoir rock is an essential parameter for evaluating the injection pressure during CO_2 injection.

Although tectonic stresses in Taiwan, which can be regarded as far field stresses, have been investigated extensively using GPS observations and tectonic data (Chang et al. 2003; Kaus et al. 2009; Hsu et al. 2010), local geological structures at a potential CO_2 injection site govern the local stresses in the rock mass to a considerable degree (Goodman 1989; Wu et al. 2004; Do et al. 2017). Hydraulic fracturing (HF) and overcoring (OC) are conventional techniques used in Taiwan to measure *in situ* stresses (Fig. 2). However, Villaescusa et al. (2002) noted that HF and OC techniques are time-consuming, very expensive and require specialized personnel. Additionally, OC cannot be used where no underground access is available and HF generates fractures in

* *Corresponding author*
E-mail: jhwu@mail.ncku.edu.tw

the rock mass that may damage the sealing geologic structure of the CO_2 storage site.

Acoustic emission (AE) and deformation rate analysis (DRA) are new methods to measure *in situ* stresses using borehole drilling cores. When the compressive stress applied to the rock exceeds its historical maximum, the stress memory can be measured as AE (Goodman 1963) and the inelastic strain behaviour as DRA (Yamamoto et al. 1990). These techniques also carry the advantages of being inexpensive and simple. However, AE and DRA are not widely practiced because of the poor reliability of the measured *in situ* stress (Ljunggren et al. 2003).

To increase the reliability of these methods the stresses were validated as being close to those measured by HF and OC (Villaescusa et al. 2002, 2003; Tuncay and Ulusay 2008). However, to date, a number of aspects remain problematic, such as (1) the applicability of AE and DRA to different rock types; (2) influence of delay time on the pre-stress evaluation accuracy in a specimen, with delay time representing the elapsed time from borehole drilling to the pre-stress tests in the laboratory; and (3) the impact of temperature change due to geothermic gradient (Goodman 1963; Li and Nordlund 1993; Seto et al. 2001; Kramadibrata et al. 2011). When the rock core is taken from a great depth, the temperature change affects the characteristics of the cracks in the rock. Therefore, the impact of the curing temperature on the pre-stress evaluation technique accuracy must also be investigated.

The Pliocene Yutengping Sandstone in the Kueichulin Formation is a potential CO_2 storage reservoir rock at

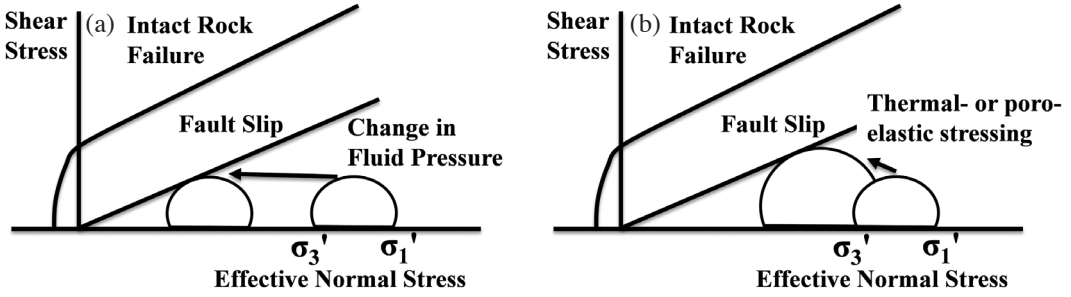

Fig. 1. Shear slip along a pre-existing fault (or fracture) during CO_2 injection (Rutqvist et al. 2007). (a) Analytical shear-slip analysis; (b) thermal- or poro-elastic stressing.

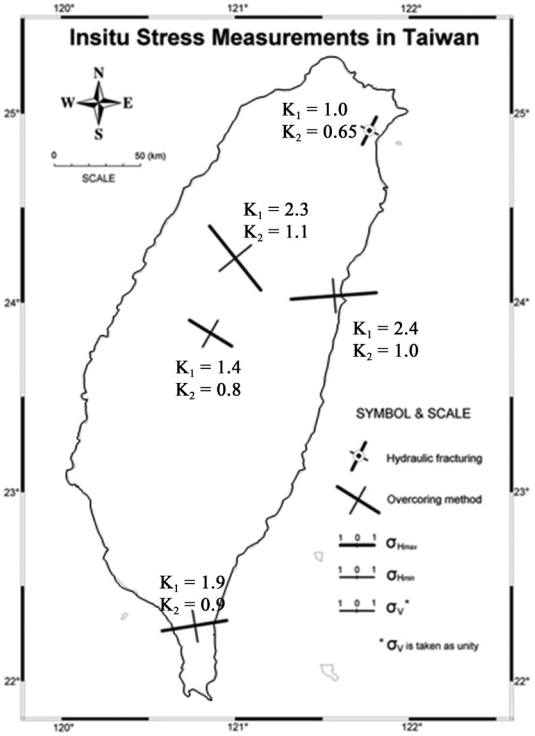

Fig. 2. *In situ* stress measurements conducted in Taiwan (Lee 2005).

Tieh-chan-shan (Lu et al. 2008). The AE and DRA techniques were applied to samples from the Yutengping Sandstone for the first time. Recent borehole drilling cores are unavailable. Therefore, instead of measuring the *in situ* stress of Yutengping Sandstone at Tieh-chan-shan, we investigate the stress memory phenomenon in rock samples from outcrops by conducting thorough laboratory tests with the following objectives: (1) to identify applicability of AE and DRA on Yutengping Sandstone and (2) to quantify the influences of the pre-stress level, the delay time and the curing temperature on the pre-stress evaluation accuracy. The *in situ* stress memorization process can be considered as creep because the rock has been buried underground subjected to a specified stress for millions of years. Therefore, in the laboratory tests, the pre-stress can be memorized into a rock using static and dynamic approaches as creep and cyclic loads, respectively (Haimson 1978). The static stress memorization applies a specified stress applied continuously to the rock sample (Li and Nordlund 1993) but pre-stress memorization takes a long time to complete for each rock sample during the tests. Alternatively, the dynamic stress memorization applies cyclic loads to the rock sample and is an alternative approach to remember the artificial pre-stress within a short experimental time. Therefore, artificial pre-stresses are applied to each sample in this study using uniaxial cyclic loads (Seto et al. 2002; Wu and Jan 2010).

2. GEOLOGIC BACKGROUND

Tieh-chan-shan is a major geologic structure and a potential geologic CO_2 storage site (Table 1) located in northwest Taiwan. The Tieh-chan-shan boundaries are the

Table 1. Major geological structure of potential reservoir rocks on Taiwan (Lu et al. 2008).

Geological structure	Reservoir rock	Depth at the top of the rock (m)	Depth at the bottom of the rock (m)
Pa-Te	Yutengping Sandstone	-1632	-1924
Ping-Chen	Yutengping Sandstone	-1414	-1521
	Kuantaoshan Sandstone	-1697	-1877
	Shanfuchi Sandstone	-1877	-2099
Keng-Tzu-Kou	Yutengping Sandstone	-1147	-1304
	Kuantaoshan Sandstone	-1360	-1643
	Shanfuchi Sandstone	-1643	-1830
Hu-Kou-Yan-Mei	Yutengping Sandstone	-1142	-1478
	Kuantaoshan Sandstone	-1506	-1705
Chu-Tung	Kuantaoshan Sandstone	-687	-1057
	Shangfuchi Sandstone	-1057	-1207
	Tungkeng Formation	-1207	-2350
Pao-Shan	Yutengping Sandstone	-1249	-1616
	Kuantaoshan Sandstone	-1699	-1981
Chu-Huang-Keng	Chuhuangkeng Formation	-1263	-1985
Chin-Shui	Shangfuchi Sandstone	-789	-989
	Tungkeng Formation	-989	-1740
Ching-Tsao-Hu-Chi-Ting	Chinshui Shale	-1498	-1506
	Yutengping Sandstone	-1517	-1796
	Kuantaoshan Sandstone	-1832	-2059
Tieh-chan-shan	Yutengping Sandstone	-1495	-1697
	Kuantaoshan Sandstone	-1730	-1857
	Shangfuchi Sandstone	-1857	-1919
Pi-Sha-Tun	Yutengping Sandstone	-1565	-1727
	Kuantaoshan sandstone	-1780	-1992
Yung-Ho-Shan	Yutengping Sandstone	-1351	-1616
	Kuantaoshan Sandstone	-1658	-1888
Pa-Kua-Shan	Cholan Sandstone	-2572	-2972
Niou-Shan	Liuchunghsi 700 m Formation	-900	-990

Futoukeng Fault to the north, Tunglo Syncline and Sanyi Fault to the east, Changhua Fault to the south and the Taiwan Strait to the west (Fig. 3). The area is 13 km long and 4 km wide. The local rock mass was generated during the Miocene, Pliocene, Pleistocene and Holocene epochs. The rock formation strike is NE - SW. The Tapingting Fault is a tear fault striking at a high angle in the fold axis dividing Tieh-chan-shan into two segmented anticlines, the Tunghsiao Anticline in the north and Tieh-chan-shan Anticline in the south. The balanced cross sections (Yang et al. 2007) show that the anticlines at Tieh-chan-shan are asymmetrical. In the north section the west wing is steep, but the east wing is gentle. In the middle section the anticline is roughly symmetrical. In the south section the west wing is gentle, but the east wing is steep. Figure 4 shows the seismic interpretation cross sections of A - A' (Fig. 4a), B - B' (Fig. 4b), and C - C' (Fig. 4c) shown in Fig. 3. In Fig. 4, the solid lines are the rock formation boundaries and the dashed lines are the thrusts. The depth of each rock formation is verified by drilling cores taken from the gas wells T-38 in Fig. 4a and T-2, T-20, and T-37 in Fig. 4b. Chuang (2011) noted that based on a seismic survey, Tieh-chan-shan is composed of two folds slipping along the thrusts at opposite dip directions. These two folds are softly linked in the transfer zone.

Tieh-chan-shan is currently the biggest gas field and underground gas storage reservoir in Taiwan. The Miocene Talu Formation, at a depth of 2750 m below sea level (Wang et al. 2011), is the main gas production sandstone. Ts'eng et al. (2003) noted that faults cut through the gas field and generate complex geological structures. The interference test data show that the thrust that parallels the anticline axis of the Tieh-chan-shan structure is a sealing fault but that other faults are fluid connected.

In addition to the geological structure, *in situ* stress is a key issue that has been investigated at Tieh-chan-shan to guarantee the safety of the underground gas storage reservoir. Wu et al. (2008b, c) highlighted the impact of *in situ* stresses on the stability of Tieh-chan-shan to securely store natural gas and CO_2. Stresses change significantly at the interfaces of different rock formations based on the value and direction of the maximum horizontal stress, evaluated using borehole breakouts (Chen and Ding 2005). Based on the *in situ* stress investigations using the petroleum exploration and exploitation database, fluid injection into the Talu Formation has been found not to reactivate the faults at Tieh-chan-shan (Wang et al. 2011). Both Chen and Ding (2005) and Wang et al. (2011) assumed that the vertical stress is the principle stress. However, by comparing the computational results using FLAC^{3D} to the borehole deformation measured using callipers at a depth of 2700 - 2750 m, Tsai et al. (2006) indicated that the complex geological structure at Tieh-chan-shan significantly disturbs the local stress. Vertical stress may therefore not be the principle stress. Further studies are required to increase the reliability of the three-dimensional *in situ* stress data.

3. PHYSICAL AND MECHANICAL PROPERTIES OF THE YUTENGPING SANDSTONE

The Yutengping Sandstone, a rock member of the Kueichulin Formation, consists of lithic graywacke, subgraywacke and propoquartzite with intercalcated gray shale. Ripple marks, coal fragments, cross-stratifications, plant fossils and sand pipes are frequently observed in this member (Chou 1980). The Pliocene Yutengping Sandstone, at a depth of 1495 - 1697 m below the ground surface, is a potential reservoir rock for future CO_2 storage, as it may offer advantages over the well-investigated Talu Formation.

At the time of this writing recent borehole drilling cores at Tieh-chan-shan were unavailable. Some samples were taken from a rock outcropping in the eastern Tieh-chan-shan geologic structure for the AE and DRA investigations. Rock cylinders were drilled from rock blocks (Fig. 5a) with diameters of 50 mm and height-to-diameter ratios of 2-to-2.5 (as recommended by ASTM4543-04) (Fig. 5b). After sample preparation each sample was air-dried for at least 7 days. Table 2 lists the uniaxial compressive strength, water content and Young's modulus of the air-dried samples. The average uniaxial compressive strength was q_u = 8.32 MPa. The average unit weight and void ratio of the sandstone are 25.48 kN m^{-3} and 0.027, respectively. The dynamic mechanical properties of the air-dried sandstones are shown in Table 3.

4. METHODOLOGY

4.1 Acoustic Emission

AE detects the pre-stress of a material by measuring acoustic emissions as the material is loaded and, when it is reloaded (Fig. 6a), measuring the degree to which the new stress exceeds the previously applied stress, at which point the acoustic emission increases significantly (Fig. 6b). This phenomenon is called the Kaiser Effect. In ASTM E 610-77 the Kaiser Effect is defined as *the absence of detectable acoustic emission until previously applied stress levels are exceeded*. Goodman (1963) first validated that the Kaiser Effect also exists in rocks.

The mechanism and theory of the Kaiser Effect are not well known. Rock type, delay time and the level of stress govern the fracture propagations in the rock and control the accuracy of pre-stress evaluations using AE (Goodman 1963; Scholz 1968 a, b, c). Table 4 shows that some rocks even show a poor Kaiser Effect (Li and Nordlund 1993). Although the *in situ* stresses evaluated using AE are validated close to those measured using the conventional HF and OC techniques (Villaescusa et al. 2002, 2003; Tuncay and Ulusay 2008), the reliability of using AE in *in situ* stress evaluations remains low (Ljunggren et al. 2003). Therefore,

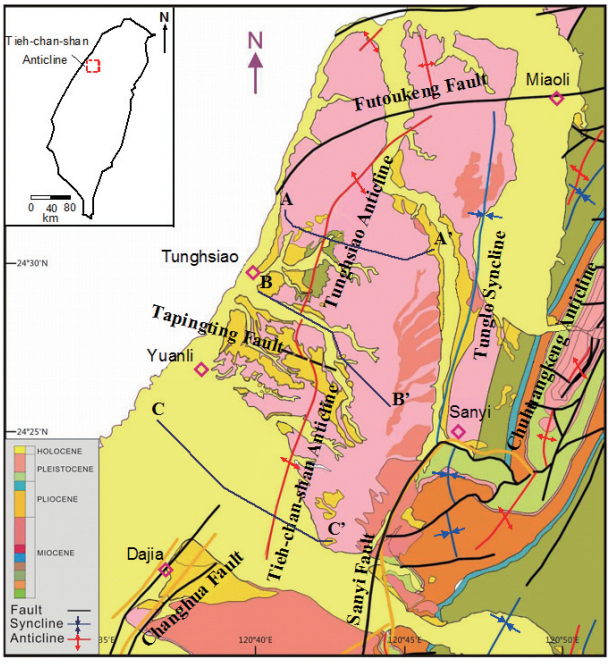

Fig. 3. Geologic map of the Tieh-chan-shan field (Chuang 2011). (Color online only)

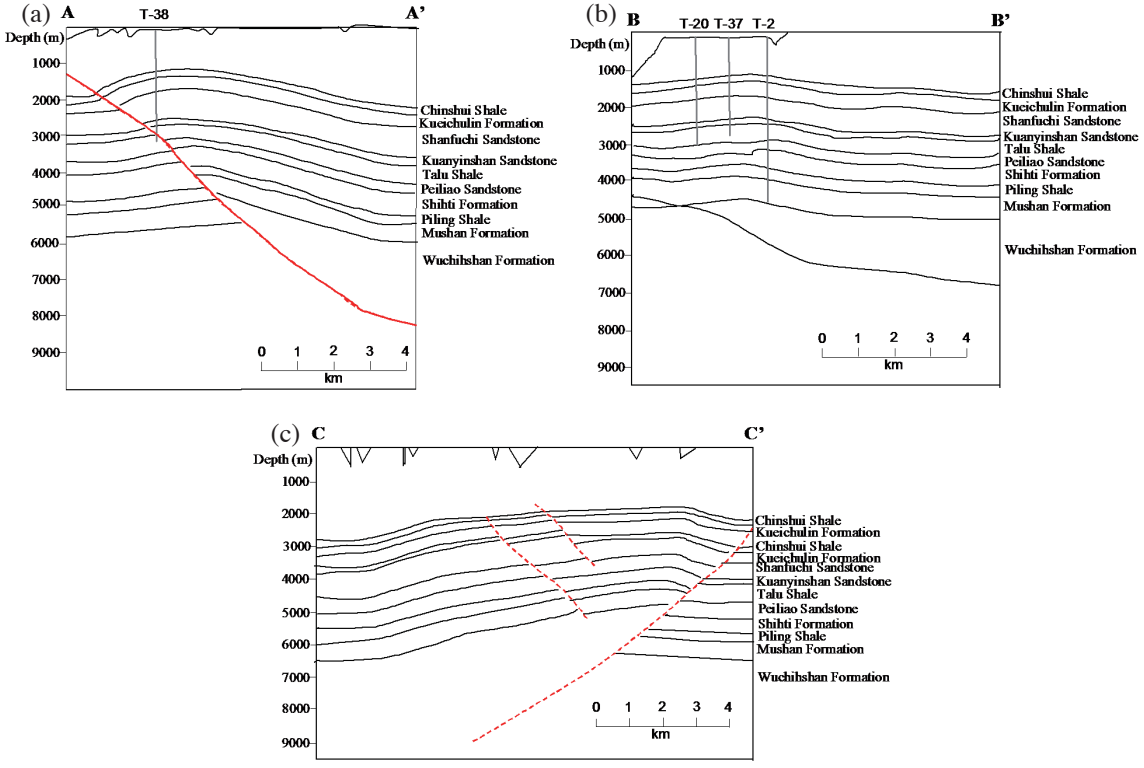

Fig. 4. Underground rock mass profiles at Tieh-chan-shan (modified from Chuang 2011). (a) A - A' profile; (b) B - B' profile; (c) C - C' profile. (Color online only)

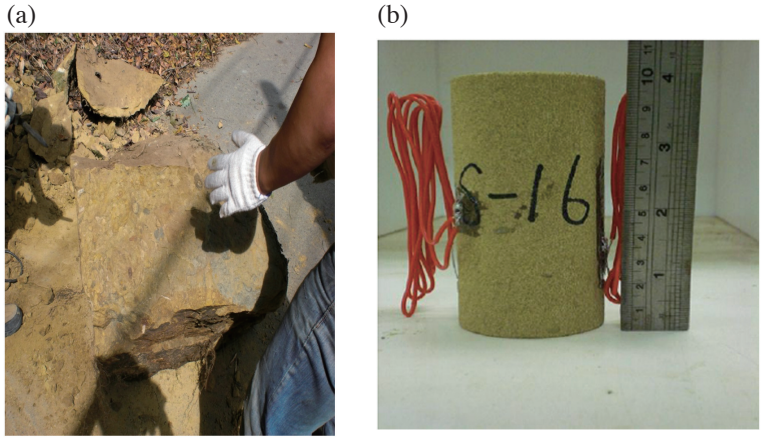

Fig. 5. Yutengping sandstone. (a) Rock at the outcrop; (b) core sample. (Color online only)

Table 2. Physical and mechanical properties of the air-dried Yutengping Sandstone.

Sample	q_u (MPa)	Water content, w (%)	Young's modulus, E (MPa)
A-1	7.22	0.98	513.83
A-2	8.36	0.93	424.46
A-3	9.38	1.26	553.82

Table 3. Dynamic mechanical properties of the Yutengping Sandstone.

Sample	Sample length (cm)	Travel time of S-wave (μsec)	S-wave velocity (m s^{-1})	Travel time of P-wave (μsec)	P-wave velocity (m s^{-1})	Dynamic Poisson's Ratio υ_d	Dynamic shear modulus G_d (MPa)	Dynamic Young's modulus E_d (MPa)
S-2	10.56	228	463.16	139	759.71	0.20	415.89	1001.66
S-6	10.46	224	466.96	137	763.50	0.20	421.74	1013.20
C-3	10.55	240	439.58	146	722.60	0.21	372.07	897.64
C-8	10.51	230	456.96	138	761.59	0.22	405.84	989.23
H-3	10.34	258	400.78	154	671.43	0.22	308.48	754.71

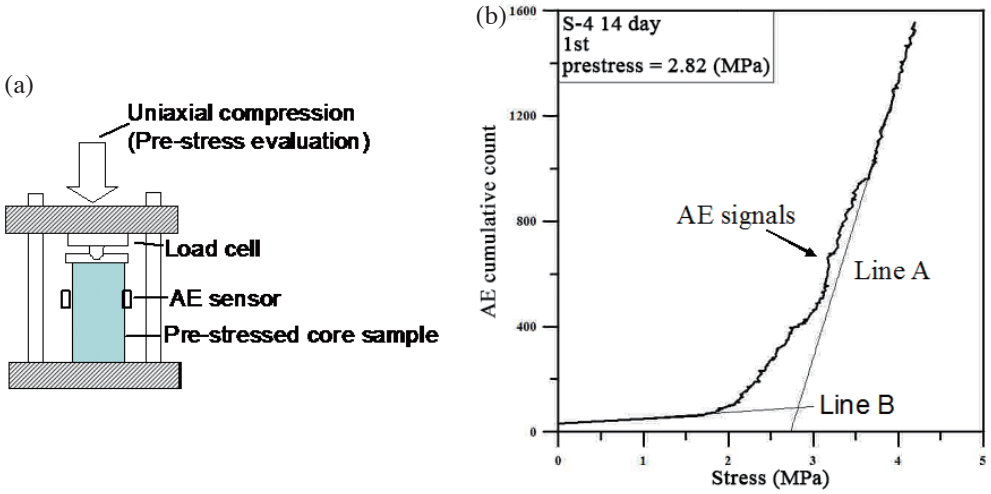

Fig. 6. Test process of pre-stress estimation using AE technique. (a) Uniaxial compressive test; (b) pre-stress interpretation. (Color online only)

Table 4. The Kaiser Effect of different rocks (Li and Nordlund 1993).

Excellent	Good	Poor
Björka marble		
Malmberget gneiss		
	Malmberget iron ore	
		KUJ iron ore
KUJ porphyry		
	Kallax gabbro	
	Luossavaara iron ore	
Luossavaara porphyry		
Zinkgruvan zinc ore		
	Viscaria greenstone	
Bolmen gneiss		
Näsliden chalcopyrite ore		
Bohus granite		
Strioa granite		

quantifying the accuracy of pre-stress AE evaluations is a key issue, especially when AE is applied to rock for the first time.

4.2 Deformation Rate Analysis

The deformation rate analysis (DRA) method is based on the deformation memory effect. This method is applies more than twice the cyclic uniaxial compressible load to pre-stressed cores (Fig. 7a) and measures the corresponding strain differences during loads (Fig. 7b). Yamamoto et al. (1990) proposed the following equation [Eq. (1)] to calculate the difference in axial strain ($\Delta\varepsilon_{ij}$) in conventional DRA:

$$\Delta\varepsilon_{ij} = \varepsilon_i(\sigma) - \varepsilon_j(\sigma);\ j > i \quad (1)$$

where, $\varepsilon_i(\sigma)$ is the axial strain at the σ stress of the ith load. The variable $\varepsilon_j(\sigma)$ is the axial strain at the σ stress of the jth load.

Yamamoto et al. (1990) noted that the strain difference function in Fig. 7b can be approximated using a straight line with a positive gradient at stresses less than the pre-stress subjected to the rock sample and it sharply bends down near the pre-stress of two successive loads. The positive gradient at the applied stresses less than the pre-stress indicates that the rock sample is more compliant under the second load than in the first load because the increase in crack density at high stresses from the first load. On the contrary, the negative gradient in the strain difference function (Fig. 7b) means that the rock is easier to deform in the first load than in second load because the rock is ready to enlarge pre-existing cracks or to create new cracks when it first experiences high applied stresses.

Uniaxial DRA successfully evaluated the *in situ* stress (Yamamoto and Yabe 2001) and correlated well with other in situ stress evaluation techniques (Seto et al. 2001; Shimada et al. 2001; Stacey and Wesseloo 2002). However, the DRA application to practical *in situ* stress evaluations is still problematic for the following reasons: (1) low reliability of pre-stress estimation, (2) unclear stress memory mechanism and (3) impacts of critical environmental factors and (4) effects of delay time on the pre-stress evaluation accuracy (Seto et al. 2001).

The pre-stress of a rock sample can be evaluated using AE and DRA simultaneously. Furthermore, the test results comparison conducted sing AE and DRA increases the evaluated pre-stress confidence. However, using both AE and DRA to detect the pre-stress of a rock is only in its preliminary stages in Taiwan. Previous work includes that of Lin et al. (2007), who investigated the AE and DRA characteristics of Mushan Sandstone; Wu et al. (2008a), who assessed the accuracy of AE in evaluating the pre-stress applied to anisotropic block schist; and Wu and Jan (2010) and Wu and Pan (2013), who evaluated the pre-stresses of Changchikeng sandstone, the main rock in the Tseng-wen Reservoir trans basin water tunnel.

Using AE and DRA for CO_2 reservoir rock storage *in situ* stress determination is very attractive for the following reasons (modified from Stacey and Wesseloo 2002):

(1) AE and DRA use original cores obtained for other purposes, such as exploration, which makes the methods cost effective.
(2) Cores obtained remotely can be used; therefore, the methods do not interrupt the borehole drilling procedure.
(3) Small cores are used for the tests. Therefore, many tests can be carried out using limited original borehole core lengths, which again makes the method cost effective. Additionally, the more cores tested the greater the confidence in the results obtained.
(4) AE and DRA do not damage the rock mass; preserving the geologic structure integrity needed to seal the CO_2 underground.

5. UNIAXIAL CYCLIC LOAD TESTING PROCEDURE FOR AE AND DRA TESTS

Samples from Yutengping Sandstone outcrops were investigated to determine the reliability of assessing the rock pre-stresses using AE and DRA. Figure 8 shows the uniaxial loading-unloading time history of our pre-stress program. The time history consists of three parts: (1) first stage of cyclic loading, (2) delay time, and (3) second stage of cyclic loading. The first stage involves 200 uniaxial 0.2 Hz load cycles to memorize pre-stress in the rock samples. Four different delay times (0, 4, 14, and 28 days) were then applied to simulate the impact of transportation time from the

in situ site to the laboratory and sample preparation because the elapsed time from the *in situ* borehole drilling to the *in situ* stress measurements is about 14 days based on personal discussions with senior engineers from CPC, Taiwan.

The Yutengping Sandstone depth at Tieh-chan-shan is between 1495 and 1697 m (Lu et al. 2008), and the sandstone unit weight is 25.48 kN m^{-3}. Therefore, the Yutenping Sandstone overburden is in the 38 - 43 MPa range, which exceeds the uniaxial compressive strength of the rock, q_u = 8.32 MPa. The maximum pre-stress for the uniaxial compressive loads is set to 5.82 MPa ($0.7q_u$). The 5.82 MPa pre-stress is certainly much less than the *in situ* overburden of 38 - 43 MPa. However, the uniaxial compressive loading is a simple approach to evaluate the possibility of conducting AE and DRA for Yutengping sandstone pre-stress assessment.

The maximum geothermal gradient at Tieh-chan-shan is 4.17°C 100 m^{-1} (Huang 1990) and the average ground temperature at Taichung, which is the nearest Central Weather Bureau temperature station is 23.3°C from 1981 to 2010 (http://www.cwb.gov.tw/V7/climate/monthlyMean/Taiwan_tx.htm). Therefore, the temperature of the Yutenping Sandstone at the depth of 1495 and 1697 m underground at Tieh-chan-shan is between 85.6 - 94.0°C. Suppose the rock cores are drilled at great depth and will be immediately subjected to unloading and a decrease in temperature once extracted. The temperature change impact on the Yutengping sandstone cores must therefore also be considered. Three curing temperatures (5, 30, and 105°C) were applied in this study to the pre-stressed samples during the delay time to investigate the impact of temperature change.

In the second cyclic load stage three uniaxial cyclic loads were applied to the samples, with AE and core deformation measured simultaneously. The P_L and P_U in the first stage (Fig. 8) are the lower and upper bounds of the cyclic load stresses, respectively. The P_U is also the pre-stress of the sample in this study. Each sample must exhibit permanent deformation after cyclic load in the first stage to guarantee successful stress ''memorization''. The maximum load (P_m in Fig. 8) in the second stage must exceed P_U in the first stage, but must not induce uniaxial compressive failure. The average uniaxial compressive strength of the sandstone was q_u = 8.32 MPa. Table 5 lists the P_L, P_U, and P_m for the

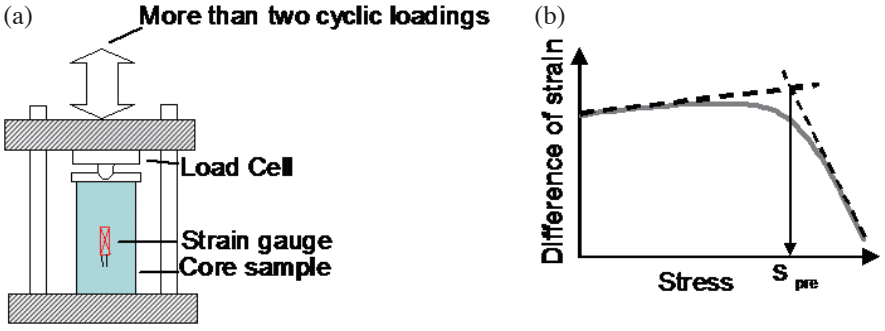

Fig. 7. Test process of pre-stress estimation by DRA. (a) Cyclic loading; (b) DRA curve. (Color online only)

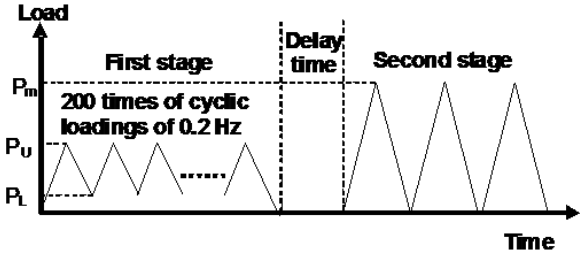

Fig. 8. Loading-unloading time history in this study.

Table 5. Applied pre-stresses on each sample.

Pre-stress	P_L	P_U	P_m
Low (MPa)	1.66 (0.2 q_u)	3.33 (0.4 q_u)	4.16 (0.5 q_u)
Medium (MPa)	2.50 (0.3 q_u)	4.16 (0.5 q_u)	4.99 (0.6 qu)
High (MPa)	4.16 (0.5 q_u)	5.82 (0.7 q_u)	6.66 (0.8 q_u)

samples used in this study.

6. PRE-STRESS EVALUATION USING ACOUSTIC EMISSION

The pre-stress applied to core samples in the first stage (Fig. 8) was assessed by measuring the AE signals from the first loading in the second stage cyclic load. When the load exceeded the previous maximum stress parallel to the load direction, significant AE signals occurred, which is known as the Kaiser Effect. The rock core axis does not necessarily coincide with the direction of any principal stress axis. Villaescusa et al. (2002) and Wu and Pan (2013) proposed algorithms to generated three-dimensional stresses using the pre-stress evaluations from oriented cores. The testing procedure (Figs. 6 and 9) is discussed below.

(1) Core drilling was conducted in Yutengping Sandstone blocks to obtain core samples (Fig. 9a).
(2) We assumed that the *in situ* stresses acting on the rock samples, which were taken from an outcrop rock block, were much lower than the specified pre-stresses in Table 5. Hence 200 uniaxial cyclic loads were applied to the cored samples to simulate the imposed pre-stress (Fig. 9b).
(3) A pre-stressed sample was installed on a loading system with two AE sensors that monitored the AE signals during the load testing (Fig. 6a). A miniature PICO sensor was selected because of its size and appropriate operation frequency, which is in the 200 - 750 kHz range (http://www.pacndt.com/index.aspx?go=products&focus=/sensors/miniature.htm). The frequency range of the geomaterials in these laboratory tests is in the 100 kHz - 1 MHz range (Scholz 1968a, b, c) and 100 Hz - 50 kHz range (Hardy 1972). The PICO sensor has a diameter of 5 mm and a height of 4 mm, and can be easily attached to the cylindrical surface of the sample. The pencil lead break technique (ASTM E976-10) was used to check for proper equipment operation.
(4) AE cumulative count versus loading stress was plotted (Fig. 6b). The pre-stress value, σ_{pre}, was obtained by projecting the tangent, Lines A and B, at the turning point suggested by Lavrov (2003).
(5) The pre-stress evaluated using the AE signals was compared with the memorized pre-stress, P_U, in Table 5.

7. PRE-STRESS EVALUATION BY DEFORMATION RATE ANALYSIS

Wu and Jan (2010) noted that both axial strain and lateral strain can be used in DRA. Therefore, three load cycles were imposed in the second cyclic loading stage to assess the pre-stress, P_U (see Fig. 8), with an axial strain gauge and a lateral strain gauge attached on opposite sides of the sample after the pre-stress memorization shown in Fig. 7a.

The basic DRA concepts are explained as follows (Seto et al. 2001):

(1) Cracks in the rock sample, which are caused by pre-stress, deform steadily under low stresses.
(2) The rock deformation rate changes when the stress applied to the rock sample exceeds the pre-stress to generate new cracks.

Figure 7b shows that the difference between strains in the cyclic loads is a curve. Therefore, in a method similar to that proposed by Lavrov (2003) for AE, tangents to the maximum curvature are used to determine the pre-stress value, σ_{pre}.

8. EXPERIMENTAL RESULTS OF THE PRE-STRESS EVALUATION

Four delay times (0, 4, 14, and 28 days) and three curing temperatures (5, 30, and 105°C) were applied to the samples during pre-stress evaluations. When the delay time = 0 days, the cyclic loads in the second stage (Fig. 8) were applied to the pre-stress samples subsequent to the cyclic loads in the first stage. When the delay time > 0 days, the pre-stress samples were placed in a chamber with a fixed curing temperature for the specified delay time minus two days. The samples were then stored at room temperature for two days before applying the cyclic loads in the second stage.

The pre-stress evaluation is successful in most Yutengping Sandstone samples using AE (Table 6). However, the AE signals in Fig. 10 bend slightly downward and are different from the conventional upward curve shown in Fig. 6b. We therefore judged that Fig. 10 fails to evaluate the pre-stress. The error in Table 6 is calculated using the following Eq. (2):

$$\text{Err}^{\circ}\text{r}(\%) = (\text{Evaluated pre - stress - } P_u) \times 100\% / P_u \qquad (2)$$

The error is positive when the estimated stress overestimates the pre-stress and negative when the estimated stress underestimates the pre-stress. The estimated stresses errors using AE are in the range from -36.04 - 15.14% (Table 6).

In conventional DRA pre-stress was estimated using the strain difference between the 2nd load and the 1st load in the second stage. However, the concave curve of the strain difference in the pre-stress sandstones (Fig. 11), which is caused by zero-stress memory (Yamamoto et al. 1990), is not the typical convex curve (Fig. 7b). Zero-stress memory can be caused due to the cracks produced during/ the cyclic loads in the first stage and destroyed by the first load in the second stage (Fig. 8) (Yamamoto et al. 1990). The typical convex DRA curve in this study was obtained using the strain difference between the 3rd load and the 2nd load in the second stage based on the suggestions by Yamamoto et al. (1990). Additionally, DRA applies uniaxial strain

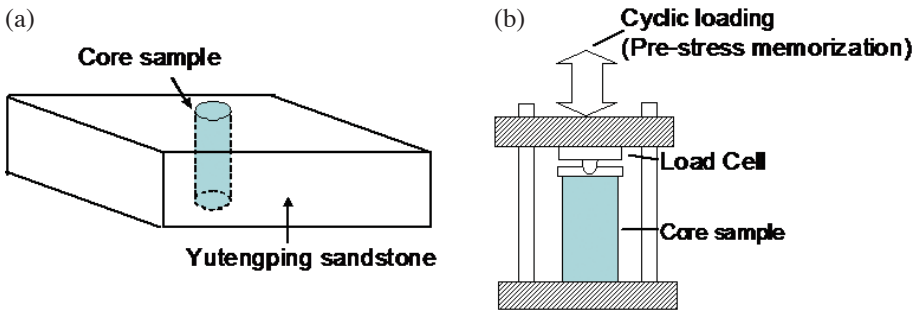

Fig. 9. Core drilling and pre-stress memorization. (a) Core drilling; (b) pre-stress memorization. (Color online only)

Table 6. Pre-stress evaluations using AE.

Curing temperature (°C)	Delay time (day)	P_u = 3.33 MPa		P_u = 4.16 MPa		P_u = 5.82 MPa	
		Evaluated stress (MPa)	Error (%)	Evaluated stress (MPa)	Error (%)	Evaluated stress (MPa)	Error (%)
5	4 day	--	--	4.04	-2.88	5.06	-13.06
	14 day	2.65	-20.42	4.00	-3.85	5.44	-6.53
	28 day	3.52	5.71	3.25	-21.88	4.60	-20.96
30	0 day	3.14	-5.71	4.79	15.14	5.86	0.69
	0 day	3.00	-9.91	4.28	2.88	5.38	-7.56
	4 day	3.46	3.90	4.32	3.85	4.90	-15.81
	14 day	2.82	-15.32	4.4	5.77	5.84	0.34
	28 day	3.49	4.80	4.51	8.41	4.66	-19.93
105	4 day	3.22	-3.30	3.44	-17.31	4.23	-27.32
	14 day	2.13	-36.04	3.32	-20.19	5.44	-6.53
	28 day	3.01	-9.61	3.18	-23.56	--	--

Note: --: fail to evaluate the pre-stress using AE data.

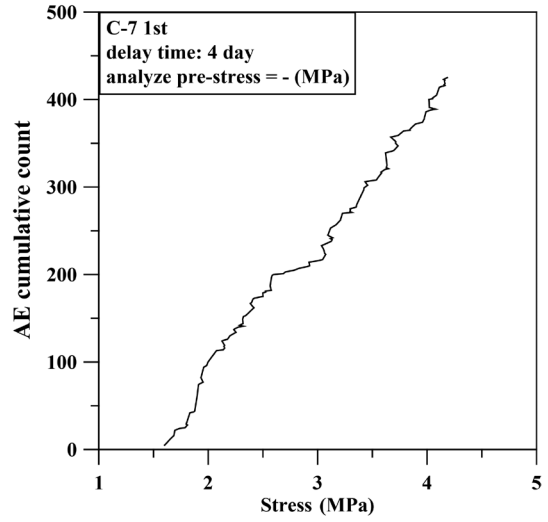

Fig. 10. Fail to evaluate pre-stress using AE.

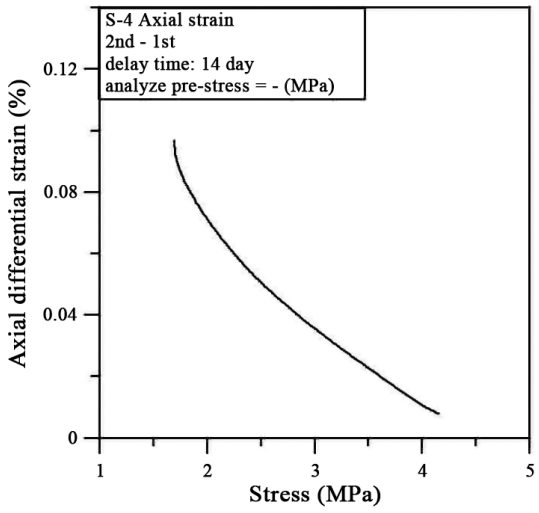

Fig. 11. Concave DRA curve.

(conventional DRA) and lateral strain to evaluate the rock pre-stress (Table 7). The estimated pre-stress errors range from -19.93 - 17.42%.

The data in Tables 6 and 7 show that many pre-stress evaluations under-estimate the pre-stresses applied to the sandstone samples by AE and overestimate the pre-stresses with DRA. The pre-stress underestimation mechanisms by AE and over-estimation by DRA are explained as follows:

(1) AE is very sensitive to the crack propagation in the rock sample. The crack distribution and characteristics in rocks is complex with tiny crack propagations that occur before the pre-stress contributing to the underestimation.

(2) In DRA the pre-stress is detected by the significant change in deformation in the rock sample. The strain difference in this study was calculated between the 3rd load and the 2nd load in the second stage. The first load in the second stage destroys the zero-stress memory (Yamamoto et al. 1990) and causes new cracks resulting in the pre-stress overestimation because the 1st load in the second stage exceeds the maximum stress of the loads in the first stage (Lin et al. 2006).

8.1 Impact of Different Delay Times and Pre-Stresses

Pre-stress evaluated using AE with a curing temperature of 30°C shows insignificant trends under different delay times and pre-stresses (Fig. 12a). The turning point in the AE curve is indistinct. Developing new methodologies to increase the pre-stress estimation accuracy with AE is essential for future studies.

In DRA the pre-stress evaluations with a curing temperature of 30°C shows that the stress memory fades as the delay time increases in both the axial strain (Fig. 12b) and the lateral strain (Fig. 12c).

8.2 Impact of Different Curing Temperature

Curing temperature does not significantly affect the pre-stress evaluations using AE (Fig. 13). Again, to increase the pre-stress evaluation accuracy further studies are required to

Table 7. Pre-stress evaluations using DRA.

Strain	Delay time (day)	P_u = 3.33MPa		P_u = 4.16MPa		P_u = 5.82MPa	
		Evaluated Stress (MPa)	Error (%)	Evaluated Stress (MPa)	Error (%)	Evaluated Stress (MPa)	Error (%)
Curing temperature = 5°C							
Axial	4	3.77	13.21	4.37	5.05	6.22	6.87
	14	3.66	9.91	4.23	1.68	5.92	1.72
	28	3.46	3.90	4.00	-3.85	5.26	-9.62
Lateral	4	3.81	14.41	4.47	7.45	6.03	3.61
	14	3.74	12.31	4.46	7.21	5.79	-0.52
	28	3.69	10.81	4.49	7.93	5.74	-1.37
Curing temperature = 30°C							
Axial	0	3.56	6.91	4.64	11.54	5.68	-2.41
	0	3.87	16.22	4.58	10.10	5.27	-9.45
	4	3.77	13.21	4.37	5.05	6.03	3.61
	14	3.66	9.91	4.23	1.68	5.92	1.72
	28	3.46	3.90	4.00	-3.85	5.26	-9.62
Lateral	0	3.76	12.91	4.63	11.30	5.76	-1.03
	0	3.91	17.42	4.56	9.62	5.68	-2.41
	4	3.81	14.41	4.47	7.45	6.03	3.61
	14	3.74	12.31	4.46	7.21	5.79	-0.52
	28	3.69	10.81	4.49	7.93	5.74	-1.37
Curing temperature = 105°C							
Axial	4	3.85	15.62	4.59	10.34	5.47	-6.01
	14	3.72	11.71	4.52	8.65	5.82	0
	28	3.36	0.90	4.19	0.72	4.66	-19.93
Lateral	4	3.80	14.11	4.37	5.05	5.72	-1.72
	14	3.25	-2.40	4.19	0.72	5.89	1.20
	28	3.50	5.12	4.14	-0.48	5.65	-2.92

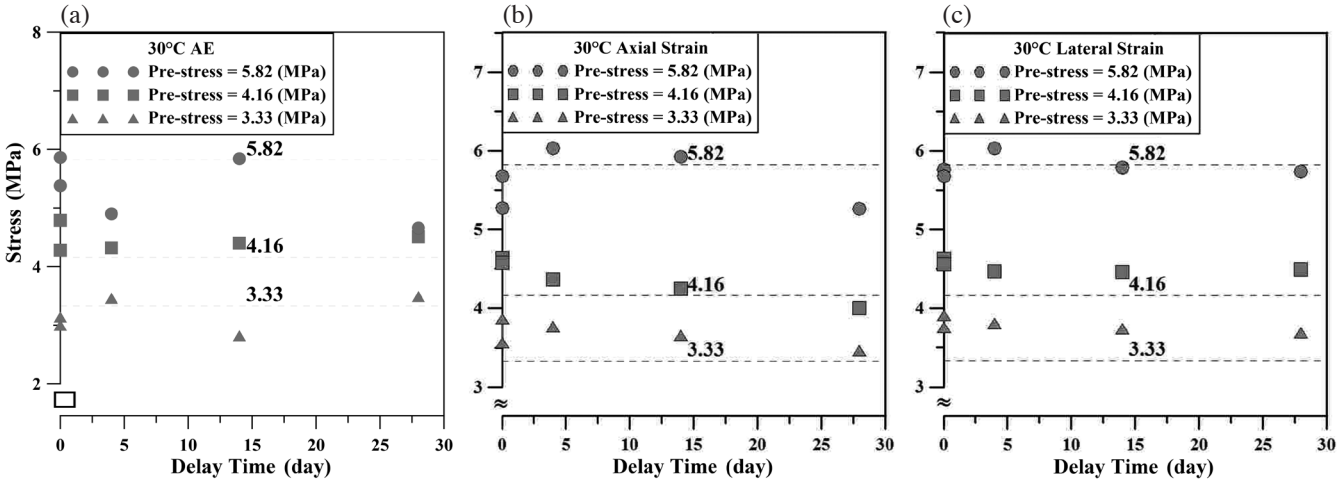

Fig. 12. Pre-stress evaluations under different delay times and pre-stresses. (a) AE; (b) DRA-axial; (c) DRA-lateral.

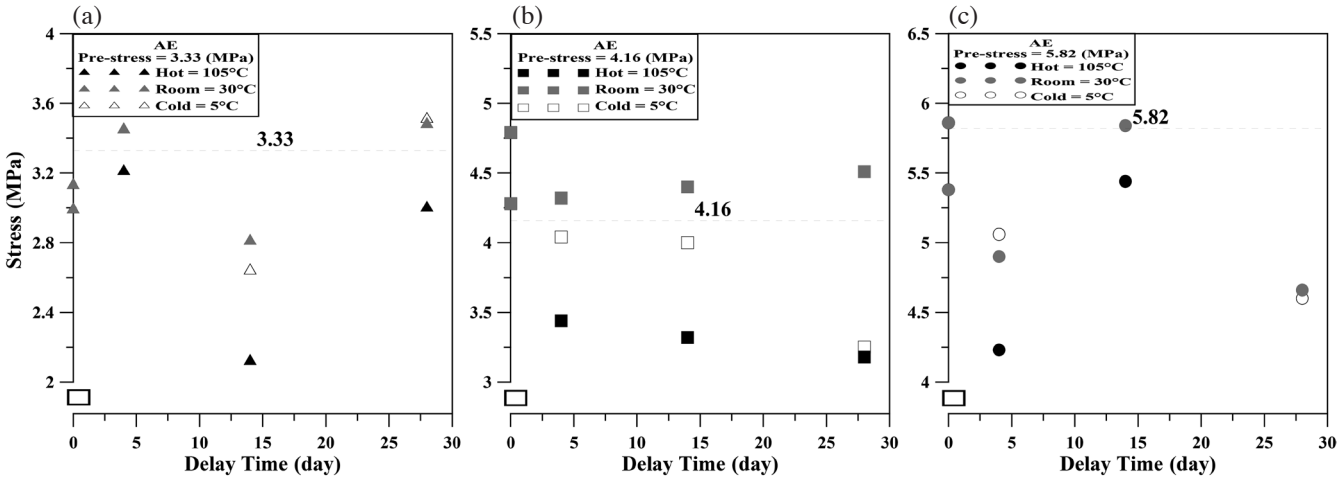

Fig. 13. Pre-stress evaluations under different curing temperature by AE. (a) Low pre-stress; (b) medium pre-stress; (c) high pre-stress.

discuss the techniques that determine the sample pre-stress and the crack distributions in the pre-stressed rocks.

The sandstone pre-stress evaluation using DRA is governed by delay time (Figs. 14 and 15). That is, in DRA studies, stress memory fades as the delay time increases. Although the temperature change may generate new cracks in the rock sample, curing temperatures from 5 - 105°C have a very minor impact on the pre-stress evaluation accuracy.

Based on Amadei and Stephansson (1997), 10 - 20% scatter in magnitude is expected in a series of pre-stress measurements in typical rock conditions. Although the maximum error in AE is -36.04% (Table 6), in this study, most data are less than 20%. In addition, the magnitude error in DRA pre-stress evaluations scatters is less than 20%. Therefore, this study validates that both AE and DRA are useful techniques to evaluate the *in situ* stress of Yutengping Sandstone with acceptable accuracy. However, although Chen (2000) noted that the high pre-stress in a rock can also be investigated under high triaxial stresses, further studies must be conducted to investigate the impact of confining pressure on pre-stress evaluation accuracy using AE and DRA since the assumed pre-stress in this study is far below the *in situ* overburden.

9. CONCLUSIONS

Uniaxial cyclic load tests validate that AE and DRA are useful tools to evaluate pre-stresses in Yutengping Sandstone. Pre-stresses are underestimated in many AE processed samples because AE is very sensitive to crack propagation in the rock sample. Delay time and curing temperature have insignificant impacts on the pre-stress estimations. Remarkable crack propagation causes changes in rock deformation resulting in DRA overestimating the pre-stress. Both axial strain and lateral strain can be used in DRA. The stress memory of Yutengping Sandstone fades as the delay

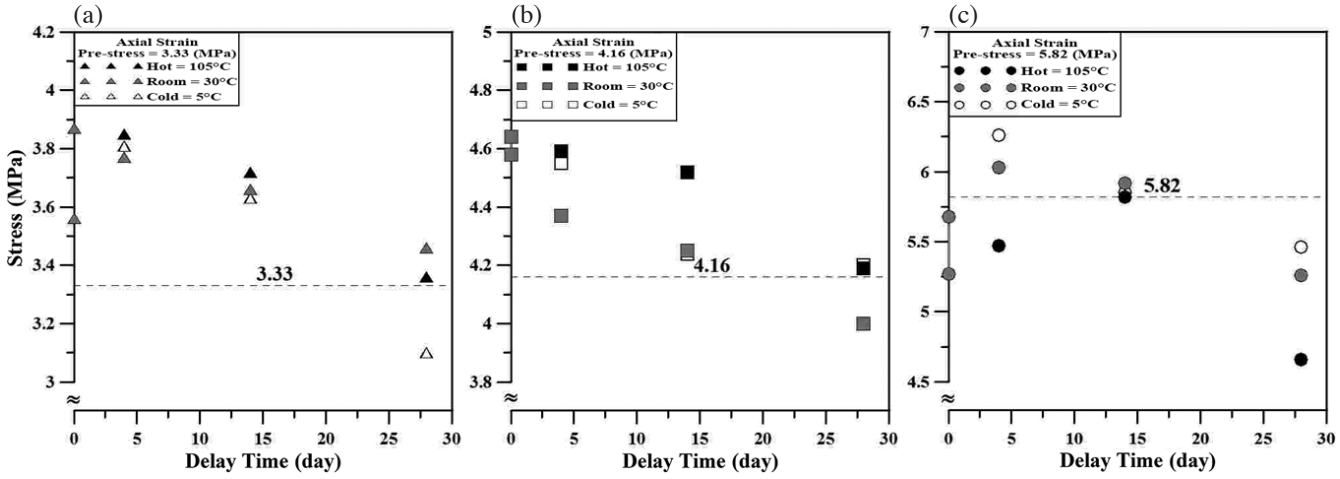

Fig. 14. Pre-stress evaluations under different curing temperature by DRA (axial strain). (a) Low pre-stress; (b) medium pre-stress; (c) high pre-stress.

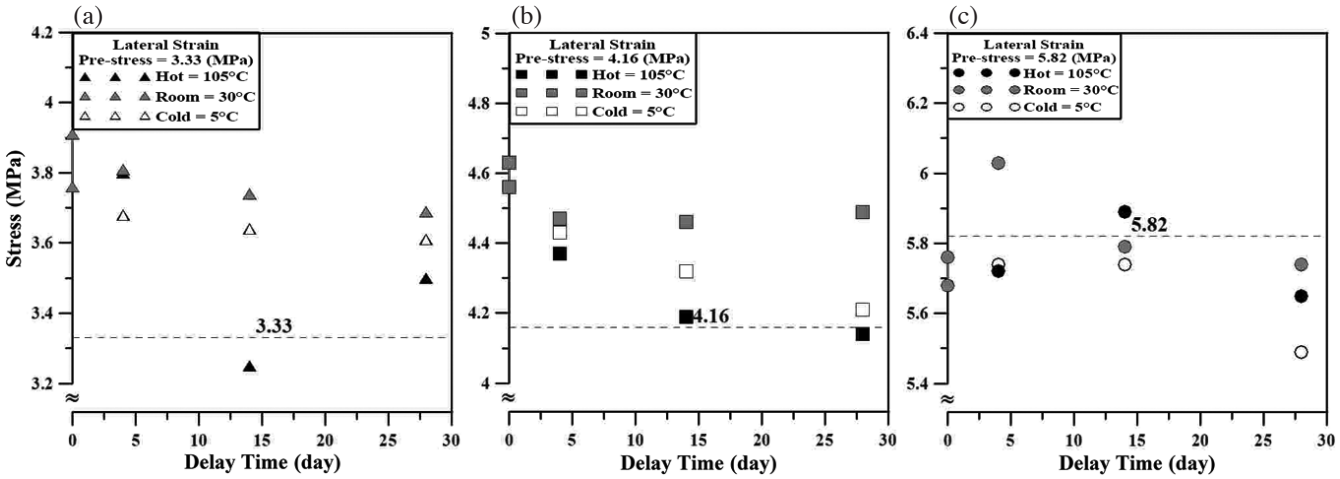

Fig. 15. Pre-stress evaluations under different curing temperature by DRA (lateral strain). (a) Low pre-stress; (b) medium pre-stress; (c) high pre-stress.

time increases. Curing temperatures between 5 - 105°C have a very minor impact on the pre-stress evaluation accuracy.

Special attention must be paid to the sample preparation, experimental procedure to increase the experimental results reliability when we practically apply AE and DRA to measure three-dimensional in-situ stresses. Samples must be drilled at different directions because AE and DRA evaluate the rock sample pre-stress parallel to the load direction. The rock sample fails before the pre-stress level when the in-situ stresses exceed the rock's uniaxial compressive strength. The triaxial compressive test increases the rock's compressive strength and may be an alternative procedure for in-situ stress measurements using AE and DRA. However, the unclear impact of confining pressure on the pre-stress evaluation accuracy and the requirement for waterproof techniques under high confining pressure to the strain gauge and AE sensors complicate the pre-stress evaluation procedure. The in-situ stresses evaluated using AE and DRA must compare to the experimental results obtained by conventional techniques to increase the data reliability.

Acknowledgements The authors would like to thank the National Science Council of Taiwan for its financial support of this research (NSC 98-3114-E-008-003 and NSC 100-3113-E-008-002) and the valuable suggestions from the Reviewers. Special appreciation is given to the CPC engineers and our colleagues at the Department of Earth Sciences and Department of Resources Engineering, National Cheng Kung University, Taiwan. The technical support from PAC and MTS is also appreciated.

REFERENCES

Amadei, B. and O. Stephansson, 1997: Rock Stress and

Its Measurement, University of Colorado Boulder, Boulder, United States of America, 490 pp, doi: 10.1007/978-94-011-5346-1. [Link]

Cailly, B., P. Le Thiez, P. Egermann, A. Audibert, S. Vidal-Gilbert, and X. Longaygue, 2005: Geological storage of CO_2: A state-of-the-art of injection processes and technologies. *Oil Gas Sci. Tech.*, **60**, 517-525, doi: 10.2516/ogst:2005034. [Link]

Chang, C. P., T. Y. Chang, J. Angelier, H. Kao, J. C. Lee, and S. B. Yu, 2003: Strain and stress field in Taiwan oblique convergent system: constraints from GPS observation and tectonic data. *Earth Planet. Sci. Lett.*, **214**, 115-127, doi: 10.1016/S0012-821X(03)00360-1. [Link]

Chen, C. H. and Y. Ding, 2005: Analyzing the stresses of the rock mass of underground gas storage reservoir using FLAC3D. 2nd Conference of Resources Engineering in Taiwan, Tainan City, Taiwan, 460-465. (in Chinese)

Chen, S. C., 2000: The AE characteristics of rocks under tri-axial stresses. Master Thesis, National Cheng Kung University, Tainan City, Taiwan, 124 pp.

Chou, J. T., 1980: Stratigraphy and sedimentology of the Miocene in western Taiwan. *Petrol. Geol. Taiwan*, **17**, 33-52.

Chuang, B. I., 2011: 3-D geometry analysis of subsurface geological structure of Tiehchanshan area, northwestern Taiwan. Master Thesis, Department of Earth Sciences, National Cheng Kung University, Tainan City, Taiwan, 81 pp.

Do, T. N., J. H. Wu, and H. M. Lin, 2017: Investigation of sloped surface subsidence during inclined seam extraction in a jointed rock mass using discontinuous deformation analysis. *Int. J. Geomech.*, **17**, doi: 10.1061/(ASCE)GM.1943-5622.0000894. [Link]

Goodman, R. E., 1963: Subaudible noise during compression of rocks. *Geol. Soc. Am. Bull.*, **74**, 487-490, doi: 10.1130/0016-7606(1963)74[487:SNDCOR]2.0.CO;2. [Link]

Goodman, R. E., 1989: Introduction to Rock Mechanics, 2th Edition, Wiley, 576 pp.

Haimson, B. C., 1978: Effect of Cyclic Loading on Rock, Dynamic Geotechnical Testing, ASTM STP 654, 228-245, doi: 10.1520/STP35679S. [Link]

Hardy, H. R., 1972: Application of Acoustic Emission Techniques to Rock Mechanics Research, Acoustic Emission, ASTM STP 505, 41-83, doi: 10.1520/STP35381S. [Link]

Hsu, Y. J., L. Rivera, Y. M. Wu, C. H. Chang, and H. Kanamori, 2010: Spatial heterogeneity of tectonic stress and friction in the crust: new evidence from earthquake focal mechanisms in Taiwan. *Geophys. J. Int.*, **182**, 329-342, doi: 10.1111/j.1365-246X.2010.04609.x. [Link]

Huang, L. S., 1990: Preliminary study on the subsurface temperature and geothermal gradients of the late Cenozoic basin in western Taiwan. *Bull. Central Geol. Surv.*, **6**, 117-144.

Kaus, B. J. P., Y. Liu, T. W. Becker, D. A. Yuen, and Y. Shi, 2009: Lithospheric stress-states predicted from long-term tectonic models: Influence of rheology and possible application to Taiwan. *J. Asian Earth Sci.*, **36**, 119-134, doi: 10.1016/j.jseaes.2009.04.004. [Link]

Kramadibrata, S., G. M. Simangunsong, K. Matsui, and H. Shimada, 2011: Role of acoustic emission for solving rock engineering problems in Indonesian underground mining. *Rock Mech. Rock Eng.*, **44**, 281-289, doi: 10.1007/s00603-010-0125-2. [Link]

Lavrov, A., 2003: The Kaiser effect in rocks: Principles and stress estimation techniques. *Int. J. Rock Mech. Min. Sci.*, **40**, 151-171, doi: 10.1016/S1365-1609(02)00138-7. [Link]

Lee, C. T., 2005: Tectonic activity and hazards in Taiwan. Forum of Nuclear Energy and Final Disposal of Radioactive Wastes in Taiwan, Lungtan, Taoyuan City, Taiwan, 102-117.

Li, C. and E. Nordlund, 1993: Experimental verification of the Kaiser effect in rocks. *Rock Mech. Rock Eng.*, **26**, 333-351, doi: 10.1007/BF01027116. [Link]

Lin, H. M., J. H. Wu, and D. H. Lee, 2006: Evaluating the pre-stress of Mu-Shan sandstone using acoustic emission and deformation rate analysis. In: Lu, M., C. C. Li, H. Kørholt, and H. Dahle (Eds.), Proceedings of the International Symposium on In-situ Rock Stress, Taylor and Francis Group, London, 215-222, doi: 10.1201/9781439833650-29. [Link]

Lin, W., E. C. Yeh, H. Ito, T. Hirono, W. Soh, C. H. Wang, K. F. Ma, J. H. Hung, and S. R. Song, 2007: Preliminary results of stress measurement using drill cores of TCDP hole-A: An application of anelastic strain recovery method to three-dimensional in-situ stress determination. *Terr. Atmos. Ocean. Sci.*, **18**, 379-393, doi: 10.3319/TAO.2007.18.2.379(TCDP). [Link]

Ljunggren, C., Y. Chang, T. Janson, and R. Christiansson, 2003: An overview of rock stress measurement methods. *Int. J. Rock Mech. Min. Sci.*, **40**, 975-989, doi: 10.1016/j.ijrmms.2003.07.003. [Link]

Lu, M. T., T. H. Hsiuan, Y. J. Huang, and C. H. Fan, 2008: Potential estimate of geological storage for CO_2 onshore Taiwan. *Min. Metallu.*, **52**, 154-161. (in Chinese)

Rutqvist, J., J. Birkholzer, F. Cappa, and C. F. Tsang, 2007: Estimating maximum sustainable injection pressure during geological sequestration of CO_2 using coupled fluid flow and geomechanical fault-slip analysis. *Energ. Convers. Manage.*, **48**, 1798-1807, doi: 10.1016/j.enconman.2007.01.021. [Link]

Scholz, C. H., 1968a: The frequency-magnitude relation of microfracturing in rock and its relation to earthquakes. *Bull. Seismol. Soc. Am.*, **58**, 399-415.

Scholz, C. H., 1968b: Microfracturing and the inelastic

deformation of rock in compression. *J. Geophys. Res.*, **73**, 1417-1432, doi: 10.1029/JB073i004p01417. [Link]

Scholz, C. H., 1968c: Experimental study of the fracturing process in brittle rock. *J. Geophys. Res.*, **73**, 1447-1454, doi: 10.1029/JB073i004p01447. [Link]

Seto, M., N. Soma, N. Meada, H. Matsui, E. Villaescusa, and K. Katsuyama, 2001: Methodology and case studies of stress measurement by the AE and DRA methods using rock core. *Shigen-to-Sozai*, **117**, 829-835, doi: 10.2473/shigentosozai.117.829. (in Japanese) [Link]

Seto, M., M. Utagawa, and K. Katsuyama, 2002: Some fundamental studies on the AE method and its application to in-situ stress measurements in Japan. 5th International Workshop on the Application of Geophysics in Rock Engineering, Toronto, 67-71.

Shimada, H., F. Goto, M. Seto, and K. Matsui, 2001: Fundamental study on applicability on in-situ stress using DRA method. *Shigen-to-Sozai*, **117**, 202-208, doi: 10.2473/shigentosozai.117.202. (in Japanese) [Link]

Stacey, T. R. and J. Wesseloo, 2002: Application of indirect stress measurement techniques (non strain gauge based technology) to quantify stress environments in mines. Final Project Report, No. GAE/858, The University of the Witwatersrand & SRK Consulting, 67 pp.

Streit, J. E. and R. R. Hillis, 2004: Estimating fault stability and sustainable fluid pressures for underground storage of CO_2 in porous rock. *Energy*, **29**, 1445-1456, doi: 10.1016/j.energy.2004.03.078. [Link]

Tsai, S. H., M. W. Tang, and Y. Ding, 2006: Investigation of the stress distribution impact by the geologic structures at TCS. Taiwan Rock Engineering Symposium, Tainan City, Taiwan, 259-268. (in Chinese)

Ts'eng, C. C., W. J. Wu, and T. L. Chen, 2003: Study of fault-sealing problems in the structure of TCS. *Petrol. Geol. Taiwan*, **36**, 215-240. (in Chinese)

Tuncay, E. and R. Ulusay, 2008: Relation between Kaiser effect levels and pre-stresses applied in the laboratory. *Int. J. Rock Mech. Min. Sci.*, **45**, 524-537, doi: 10.1016/j.ijrmms.2007.07.013. [Link]

Villaescusa, E., M. Seto, and G. Baird, 2002: Stress measurements from oriented core. *Int. J. Rock Mech. Min. Sci.*, **39**, 603-615, doi: 10.1016/S1365-1609(02)00059-X. [Link]

Villaescusa, E., C. R. Windsor, J. Li, G. Baird, and M. Seto, 2003: Experimental verification of AE in situ stress measurements. 3rd International Symposium on Rock Stress, Kumamoto, Japan, 395-402.

Wang, L. J., J. H. Hung, J. J. Dong, and B. Y. Wu, 2011: In-situ stress field and fault reactivation in the Tienchanshan field, west-central Taiwan. *Min. Metallu.*, **55**, 69-82. (in Chinese)

Wu, J. H. and S. C. Jan, 2010: Experimental validation of core-based pre-stress evaluations in rock: A case study of Changchikeng sandstone in the Tseng-wen reservoir transbasin water tunnel. *Bull. Eng. Geol. Environ.*, **69**, 549-559, doi: 10.1007/s10064-010-0265-3. [Link]

Wu, J. H. and Y. W. Pan, 2013: Three-dimensional in situ stress evaluation using a new under-coring technique: the Tseng-Wen reservoir transbasin water tunnel. *Environ. Earth Sci.*, **68**, 77-86, doi: 10.1007/s12665-012-1717-9. [Link]

Wu, J. H., Y. Ohnishi, and S. Nishiyama, 2004: Simulation of the mechanical behavior of inclined jointed rock masses during tunnel construction using discontinuous deformation analysis (DDA). *Int. J. Rock Mech. Min. Sci.*, **41**, 731-743, doi: 10.1016/j.ijrmms.2004.01.010. [Link]

Wu, J. H., C. F. Chan, and S. L. Lai, 2008a: Investigating the precision of deformation rate analysis on anisotropic rock. *J. Taiwan Soc. Public. Works*, **4**, 31-39. (in Chinese)

Wu, M. S., C. C. Hu, C. Y. Wang, and K. H. Chang, 2008b: Inference of the gas-oil ratio distribution on Tiehchenshan and Chinshui-Yuanhoshan hydrocarbon migration routes. *Min. Metallu.*, **52**, 143-150. (in Chinese)

Wu, M. S., C. C. Hu, J. H. Chiu, and S. H. Wu, 2008c: Migration mechanism of the hydrocarbon in the Tiehchenshan structure. *Min. Metallu.*, **52**, 162-179. (in Chinese)

Yamamoto, K. and Y. Yabe, 2001: Stresses at sites close to the Nojima Fault measured from core samples. *Isl. Arc*, **10**, 266-281, doi: 10.1111/j.1440-1738.2001.00325.x. [Link]

Yamamoto, K., Y. Kuwahara, N. Kato, and T. Hirasawa, 1990: Deformation rate analysis: A new method for in situ stress estimation from inelastic deformation of rock samples under uni-axial compressions. *Tohoku Geophy. Journ.*, **33**, 127-147.

Yang, K. M., S. T. Huang, J. C. Wu, H. H. Ting, W. W. Mei, M. Lee, H. H. Hsu, and C. J. Lee, 2007: 3D geometry of the Chelungpu thrust system in central Taiwan: Its implications for active tectonics. *Terr. Atmos. Ocean. Sci.*, **18**, 143-181, doi: 10.3319/TAO.2007.18.2.143(TCDP). [Link]